

# Efficiency Enhancement and Beam Shaping of GaN–InGaN Vertical-Injection Light-Emitting Diodes via High-Aspect-Ratio Nanorod Arrays

Min-An Tsai, Peichen Yu, *Member, IEEE*, C. L. Chao, C. H. Chiu, H. C. Kuo, *Senior Member, IEEE*, S. H. Lin, J. J. Huang, *Senior Member, IEEE*, T. C. Lu, *Member, IEEE*, and S. C. Wang, *Life Member, IEEE*

**Abstract**—The enhanced light extraction and collimated output beam profile from GaN–InGaN vertical-injection light-emitting diodes (VI-LEDs) are demonstrated utilizing high-aspect-ratio nanorod arrays. The nanorod arrays are patterned by self-assembled silica spheres, followed by inductively coupled-plasma reactive ion etching. The fabricated nanorod arrays not only provide an omnidirectional escaping zone for photons, but also serve as waveguiding channels for the emitted light, resulting in a relatively collimated beam profile. The light output power of the VI-LED with nanorod arrays is enhanced by 40%, compared to a conventional VI-LED. The measured far-field profiles indicate that the enhancement is mainly along the surface normal direction, within a view angle of 20°.

**Index Terms**—Beam shaping, GaN, high-aspect-ratio nanorod arrays, vertical-injection light-emitting diodes (VI-LEDs).

## I. INTRODUCTION

OVER the past decade, III-nitride-based light-emitting diodes (LEDs) have been extensively studied due to widely tunable emission wavelengths ranging from ultraviolet to blue/green. High-efficiency white light LEDs using GaN–InGaN and phosphors have also received much interest for their potentials in a variety of applications, such as back lights for cell phones [1], outdoor displays [2], and most importantly, replacing incandescent or fluorescent mercury (Hg) and xenon (Xe) lamps for general lighting devices. However, a majority of applications are currently hindered by the low extraction efficiency and Lambertian-like radiation profile of conventional GaN–InGaN LEDs. A typical view angle of a conventional LED is about 120°, which is not preferable for applications such as mobile phone cameras, pocket lamps, and vehicle head lamps. Hence, it is essential to develop high-efficiency LEDs with directional radiation profiles for

next-generation lighting devices. Over the past few years, various techniques have been proposed to enhance light extraction efficiency of conventional LEDs, such as patterned sapphire substrates [3], roughened or patterned LED surfaces [4], [5], and the incorporation of highly reflective omnidirectional reflectors [6]. However, some of the proposed techniques could deteriorate the electrical properties of conventional LEDs due to the thin p-GaN top layer, limiting the depth of surface textures to ~200 nm.

In this research, we proposed a novel vertical-injection LED (VI-LED) structure, where fabricating nanorod arrays with heights over 1  $\mu\text{m}$  is possible [7], [8]. The fabrication of VI-LEDs, which combines wafer bonding and laser lift-off (LLO) techniques, results in a thick n-GaN top layer, providing an excellent platform to fabricate high-aspect-ratio nanorod arrays. The nanorod arrays are patterned by uniformly spun silica spheres, followed by inductively coupled-plasma reactive ion etching (ICP-RIE). The technique is relatively cost-effective for mass production, compared to that involving electron-beam lithography [9]. The fabricated nanorods resemble cone structures, which not only provide an omnidirectional escaping zone for photons [10], but also serve as wave-guiding channels for the emitted light, resulting in a relatively collimated beam profile.

## II. EXPERIMENTS

The fabrication schematics of a GaN–InGaN VI-LED with self-organized nanorod arrays are illustrated in Fig. 1. First, a conventional LED structure was grown on a *c*-plane sapphire substrate by metal–organic chemical vapor deposition. As shown in Fig. 1(a), the epitaxial LED structure consisted of a 30-nm-thick low-temperature grown GaN buffer layer, a 2- $\mu\text{m}$ -thick undoped GaN, and a 2- $\mu\text{m}$ -thick heavily doped n-type GaN, followed by 20 pairs of InGaN–GaN multiple quantum-wells (MQWs) with a total thickness of 0.2  $\mu\text{m}$ , and a 0.2- $\mu\text{m}$ -thick p-type GaN layer. A layer of indium–tin–oxide (ITO) with a thickness of 240 nm was then deposited on p-GaN, followed by the electron-beam deposition of Ti–Al–Ti–Au with a total thickness of 2  $\mu\text{m}$  for adhesion and as a reflective mirror after wafer bonding. Next, as illustrated in Fig. 1(b), the wafer bonding process began with the deposition of bonding metals comprising Cr–Pt–Au = 50 nm/50 nm/2000 nm on both the LED structure and the silicon wafer. These two wafers were immediately placed in contact with each other using a designed fixture to ensure uniform pressure across both wafers, followed by oven annealing at 350 °C for 30 min in the nitrogen ambient. Since silicon has a higher thermal conductivity

Manuscript received October 16, 2008. First published January 06, 2009; current version published February 04, 2009. This work was supported in part by the National Science Council in Taiwan under Grant NSC96-2221-E-009-095-MY3 and Grant NSC96-2628-E-009-017-MY3.

M.-A. Tsai, C. L. Chao, and S. H. Lin are with the Department of Electrophysics, National Chiao-Tung University, Hsinchu 30010, Taiwan. (e-mail: lin@cc.nctu.edu.tw).

P. Yu, C. H. Chiu, H. C. Kuo, T. C. Lu, and S. C. Wang are with Department of Photonics and Institute of Electro-Optical Engineering, National Chiao-Tung University, Hsinchu 30010, Taiwan. (e-mail: yup@faculty.nctu.edu.tw; hckuo@faculty.nctu.edu.tw).

J. J. Huang is with the Graduate Institute of Photonics and Optoelectronics, National Taiwan University, Taipei 10617, Taiwan.

Color versions of one or more of the figures in this letter are available online at <http://ieeexplore.ieee.org>.

Digital Object Identifier 10.1109/LPT.2008.2010556

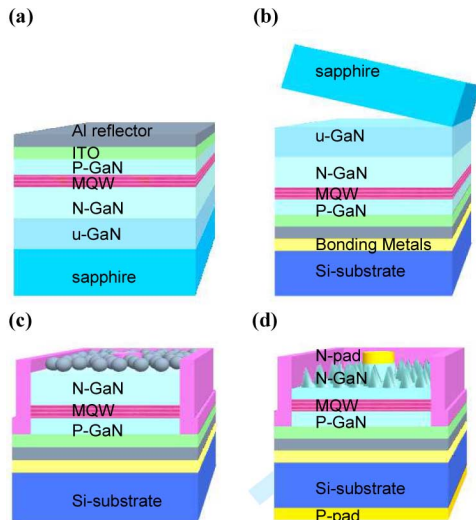


Fig. 1. Fabrication schematics of a GaN-InGaN VI-LED with self-organized nanorod arrays: (a) the epitaxial structure, (b) wafer bonding and LLO processes, (c) nanorod fabrication involving self-assembled silica spheres as lithographic and etch masks, and (d) the fabricated device schematic.

( $\sim 1.457 \text{ W/cm}^{\circ}\text{C}$ ) than that of sapphire ( $\sim 0.35 \text{ W/cm}^{\circ}\text{C}$ ) at room temperature, the host Si substrate also functions as a heat sink. After wafer-bonding, the sapphire substrate was removed by an LLO process using a KrF excimer laser (Lambda Physik LPX200) at 248-nm wavelength with a pulsewidth of 25 ns; the laser output power and beam spot size were 10 mW and  $1 \text{ mm} \times 1 \text{ mm}$ , respectively [11]. The undoped GaN was also removed by ICP-RIE. Subsequently, the mesa with an area of  $1 \times 1 \text{ mm}^2$  was defined by using standard photolithography and dry etching, and then passivated with  $\text{SiN}_x$ . As shown in Fig. 1(c), the fabrication of nanorod arrays employed self-assembled silica nanospheres as the lithographic and etch masks, which provide greater etching selectivity to n-GaN layer than other polymers. The silica spheres were first suspended in deionized (DI) water diluted in a solution of surfactant at a volume ratio of 5 : 1, and then spin-coated on the n-GaN surface, followed by heating treatment for adhesion. The surfactant can lower the surface tension and then help the particles spread across the GaN surface. The coated sample was then etched by ICP-RIE, using  $\text{Cl}_2$  and Ar as the etch gases at a fixed flow rate of 45 and 30 sccm, respectively. The device was immersed in DI water with sonification for 3 min to remove silica particles, followed by surface passivation with silicon dioxide ( $\text{SiO}_2$ ) for electric isolation. Finally, a bonding pad comprised of Cr-Pt-Au was deposited by electron-beam evaporation on the back side of Si substrate. The fabricated GaN-InGaN VI-LEDs is illustrated in Fig. 1(d).

### III. RESULTS AND DISCUSSION

Fig. 2(a) shows the field-emission scanning-electron micrograph (SEM) of the spin-coated silica spheres on GaN. The closely packed silica nanospheres have a mean diameter of 100 nm with a uniformity of better than 1%. The cross-sectional SEM image of the fabricated nanorod arrays patterned by silica spheres is shown in Fig. 2(b). These nanorods are vertically aligned to the surface normal of GaN and uniformly distributed over the entire surface. Moreover, the dense nanorod arrays exhibit uniform dimensions with a base diameter of 200 nm

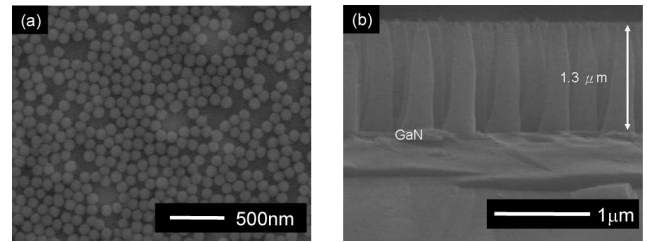


Fig. 2. Field-emission scanning-electron micrographs (FE-SEM) of (a) the densely packed silica spheres on GaN, showing a mean diameter of  $\sim 100 \text{ nm}$  with a uniformity of better than 1%; (b) the cross-sectional view of the fabricated nanorods with a base diameter of 200 nm and a height of  $1.3 \mu\text{m}$ , similar to cone structures.

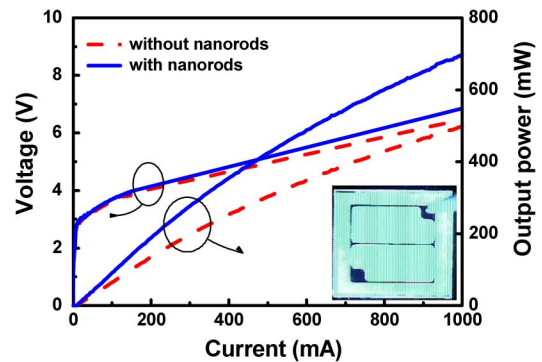


Fig. 3. Voltage and light output intensity versus forward current characteristics for a conventional GaN-InGaN VI-LED (without nanorods) and the VI-LEDs with nanorod arrays. The inset shows the uniform light emission from the VI-LEDs with nanorod arrays at a driving current of 350 mA.

and a length of  $1.3 \mu\text{m}$ , which resemble cone structures. Since the dimensions of nanorods are comparable to the emission wavelength, the spatially varied rod profiles can enhance optical transmission by collectively functioning as a gradient index layer, similar to that of a zero-order grating [12]. The enhancement in light extraction is also verified by finite-difference time-domain (FDTD) calculations.

The forward current-voltage ( $I$ - $V$ ) characteristics at room temperature for VI-LEDs with and without nanorod arrays are plotted in Fig. 3. The measured forward voltages at an injection current of 350 mA for VI-LEDs with and without nanorod arrays are 4.69 and 4.50 V, respectively. The slightly increased forward voltage for the VI-LEDs with nanorod arrays is attributed to the reduced lateral-current spreading on n-GaN, giving rise to a slightly increased resistivity. Nonetheless, both  $I$ - $V$  curves are nearly identical, indicating the negligible impact of nanorod arrays. Fig. 3 also shows the corresponding light output intensity versus forward current ( $L$ - $I$ ) characteristics. At an injection current of 350 mA, the light output power of the VI-LEDs with nanorod arrays is  $\sim 316 \text{ mW}$ , approximately enhanced by 40% compared to that without nanorods,  $\sim 226 \text{ mW}$ . The peak emission wavelength is the same as that of a conventional VI-LED, occurring at 465 nm. The inset of Fig. 3 demonstrates the uniform illumination from the VI-LEDs with nanorod arrays at a driving current of 350 mA under an optical microscope.

The measured far-field emission profiles are shown in Fig. 4(a) for VI-LEDs with and without nanorod arrays. As seen in Fig. 4(a), the emission from VI-LEDs with high-aspect-ratio nanorods is mainly enhanced along the surface normal view

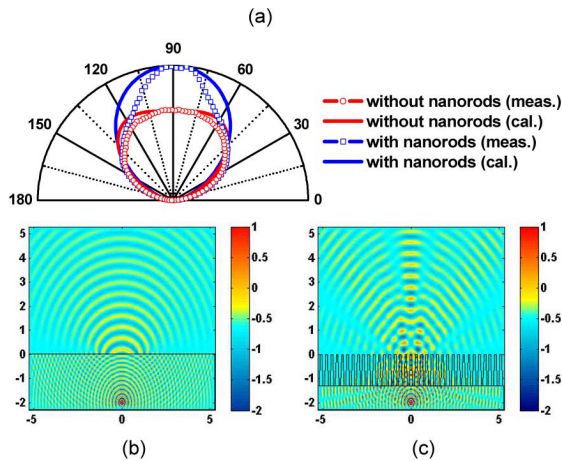


Fig. 4. (a) Measured and simulated emission profiles of a GaN–InGaN VI-LEDs with and without nanorod arrays, where the snap shots of simulated wave propagation are shown in (b) and (c), respectively.

angle of  $\pm 30^\circ$ . The integrated intensity is improved by a factor of 38% within a view angle of  $20^\circ$ . A two-dimensional FDTD method with perfectly matched layer boundary within a condition is employed to investigate the emission characteristics from high-aspect-ratio nanorod arrays. The simulated far-field patterns are plotted in Fig. 4(a) for comparison. Fig. 4(b) and (c) show the snap shots of wave propagating across a GaN–air interface and an interface with nanorod arrays, respectively. The time-varying current-excited radiation source is placed  $\sim 2 \mu\text{m}$  below the GaN–air interface. The dimensions of nanorods are extracted from the SEM picture shown in Fig. 2(b). As shown in Fig. 4(a), a conventional GaN–air interface results in Lambertian-like radiation patterns with a view angle at the full-width at half-maximum of  $\sim 120^\circ$ . The radiation pattern from the nanorod arrays is relatively collimated,  $\sim 100^\circ$ . As shown in Fig. 4(c), the nanorods suppress the total internal reflection at GaN–air interface, effectively reducing the energy confined in GaN slab. The light extraction enhancement is due to similar mechanisms provided by other surface roughness techniques. However, as shown in Fig. 4(c), the nanorods also act as waveguiding channels for the emitted light, resulting in a relatively collimated radiation pattern. Calculations show that the height of nanorods to be at least a few wavelengths long to provide a sufficient guiding effect. Moreover, the closer the nanorod array to MQWs, the better the directionality. However, the distance in this device is limited to  $\sim 1 \mu\text{m}$ , which is optimized for current spreading.

#### IV. CONCLUSION

In summary, the GaN–InGaN VI-LEDs with high-aspect-ratio nanorod arrays are demonstrated by using self-organized silica spheres for patterning, followed by ICP-RIE. The output power of a VI-LED with nanorod arrays is improved by 40% due to enhanced light extraction. Based

on the measured far-field profiles, the enhancement is mainly along the surface normal direction, within a view angle of  $20^\circ$ . We believe that VI-LEDs with high-aspect-ratio nanorod arrays offer a viable solution for efficiency enhancement and radiation profile shaping, suitable for applications in solid state lighting and displays.

#### ACKNOWLEDGMENT

The authors would like to thank Liteon Corporation for their technical support.

#### REFERENCES

- [1] Y. Narukawa, I. Niki, K. Izuno, M. Yamada, Y. Murazki, and T. Mukai, "Phosphor-Conversion white light emitting diode using InGaN near-ultraviolet chip," *Jpn. J. Appl. Phys.*, vol. 41, pp. L371–L373, 2002.
- [2] E. F. Schubert and J. K. Kim, "Solid-State light sources getting smart," *Science*, vol. 308, pp. 1274–1278, 2005.
- [3] M. R. Krames, M. Ochiai-Holcomb, G. E. Höfler, C. Carter-Coman, E. I. Chen, I.-H. Tan, P. Grillot, N. F. Gardner, H. F. Gardner, H. C. Chui, J.-W. Huang, S. A. Stockman, F. A. Kish, and M. G. Craford, "High-power truncated-inverted-pyramid  $(\text{Al}_x\text{Ga}_{1-x})_{0.5}\text{In}_{0.5}\text{P}/\text{GaP}$  light-emitting diodes exhibiting  $>50\%$  external quantum efficiency," *Appl. Phys. Lett.*, vol. 75, pp. 2365–2367, 1999.
- [4] Y. J. Lee, J. M. Hwang, T. C. Hsu, M. H. Hsieh, M. J. Jou, B. J. Lee, T. C. Lu, H. C. Kuo, and S. C. Wang, "Enhancing the output power of GaN-based LEDs grown on wet-etched patterned sapphire substrates," *IEEE Photon. Technol. Lett.*, vol. 18, no. 10, pp. 1152–1154, May 15, 2006.
- [5] T. Fujii, Y. Gao, R. Sharma, E. L. Hu, S. P. DenBaars, and S. Nakamura, "Increase in the extraction efficiency of GaN-based light-emitting diodes via surface roughening," *Appl. Phys. Lett.*, vol. 84, pp. 855–855, 2004.
- [6] T. Gessmann, H. Luo, J.-Q. Xi, K. P. Streubel, and E. F. Schubert, "Light-emitting diodes with integrated omnidirectionally reflective contacts," in *Proc. SPIE*, 2004, vol. 5366, pp. 53–61.
- [7] M. Y. Hsieh, C. Y. Wang, L. Y. Chen, T. P. Lin, M. Y. Ke, Y. W. Cheng, Y. C. Yu, C. P. Chen, D. M. Yeh, C. F. Lu, C. F. Huang, C. C. Yang, and J. J. Huang, "Improvement of external extraction efficiency in GaN-based LEDs by  $\text{SiO}_2$  nanosphere lithography," *IEEE Electron. Device Lett.*, vol. 29, no. 7, pp. 658–660, Jul. 2008.
- [8] R. H. Horng, S. H. Horng, C.-C. Yang, and D. S. Wu, "Efficiency improvement of GaN-based LEDs with ITO texturing window layers using natural lithography," *IEEE J. Quantum Electron.*, vol. 12, no. 6, pt. 1, pp. 1196–1201, Nov./Dec. 2006.
- [9] D. H. Kim, C. O. Cho, Y. G. Roh, H. Jeon, Y. S. Park, J. Cho, J. S. Im, C. Sone, Y. Park, W. J. Choi, and Q. H. Park, "Enhanced light extraction from GaN-based light-emitting diodes with holographically generated two-dimensional photonic crystal patterns," *Appl. Phys. Lett.*, vol. 87, pp. 203508–1, 2005.
- [10] C. H. Chiu, C. E. Lee, C. L. Chao, B. S. Cheng, H. W. Huang, H. C. Kuo, T. C. Lu, S. C. Wang, W. L. Kuo, C. S. Hsiao, and S. Y. Chen, "Enhancement of light output intensity by integrating ZnO nanorod arrays on GaN-based LLO vertical LEDs," *Electrochem. Solid-State Lett.*, vol. 11, pp. H84–H87, 2008.
- [11] J. T. Chu, T. C. Lu, H. H. Yao, C. C. Kao, W. D. Liang, J. Y. Tsai, H. C. Kuo, and S. C. Wang, "Laser lift-off fabrication of blue-violet GaN-based vertical cavity surface emitting lasers optically pumped at room temperature," *J. Appl. Phys.*, vol. V45, no. 4A, pp. 2556–2560, 2006.
- [12] Y. F. Huang, S. Chattopadhyay, Y. J. Jen, C. Y. Peng, T. A. Liu, Y. K. Hsu, C. L. Pan, H. C. Lo, C. H. Hsu, Y. H. Chang, C. S. Lee, K. H. Chen, and L. C. Chen, "Improved broadband and quasi-omnidirectional antireflection properties with biomimetic silicon nanostructures," *Nature Nanotech.*, vol. 2, pp. 770–774, 2007.